Novel Strategies Employing Deep Learning Techniques for Classifying Pathological Brain from MR Images

Mitrabinda Khuntia[1], Prabhat Kumar Sahu[2], Swagatika Devi[3]
Dept. of Computer Science and Engineering, ITER, S'O'A University, Bhubaneswar, India[1,2,3]

***Abstract*—Brain tumors are the most widespread as well as disturbing sickness, among a very precise expectancy of life almost in their serious structure. As a consequence, therapy planning is a critical component in enhancing the characteristics of the patient's life. Image modalities like computed tomography (CT), magnetic resonance imaging (MRI), along with ultrasound images are commonly used to assess malignancies in the brain, breast, etc. MRI scans, in evidence, are employed in this study to identify the brain tumors. The application of excellent categorization systems on Magnetic Resonance Imaging (MRI) aids in the accurate detection of brain malignancies. The large quantity of data produced through MRI scan, on the other hand, renders physical distribution of tumor and non-tumor in a given time period impossible. It does, however, come with major obstruction. As a consequence, in order to decrease human mortality, a dependable and automated categorizing approach is necessary. The enormous geological and anatomical heterogeneity of the environment surrounding the brain tumor makes automated classification of brain tumor a difficult undertaking. This paper proposes a classification of Convolutional Neural Networks (CNN) for automated brain tumour diagnosis. To study as well as compare the findings, other convolutional neural network designs such as MobileNet V2, ResNet101, and DenseNet121 are used. Small kernels are employed to carry out the more intricate architectural design. This experiment was carried out using Python and Google Colab. The weight of a neuron is characterized as minute.**

***Keywords*—Brain tumor; CT; MRI; CNN; MobileNet V2; ResNet101; DenseNet121**

I. Introduction

The process of changing an input image into an output image or image attributes is known as image processing. The primary goal of all image processing techniques is to make it simpler to visually recognize the image or item under investigation. Methods that incorporate quantitative analysis will augment the traditional visual examination of images. Anatomical segmentation of regions of interest (ROI), such as distinguishing a volume of abnormal tissue from a backdrop of normal tissue, is an important stage in the image processing pipeline. This will enable statistical examination of aspects that are not evident to human vision. Image segmentation is critical in the realm of image processing. Segmentation is vital in medical imaging for feature extraction, image measurements, and image presentation [1]. Image segmentation is the partitioning or segmentation of a digital image into comparable sections with the primary goal of simplifying the image under review into something more understandable and simpler to visually evaluate. Image segmentation techniques are classed as thresholding, region-based, supervised, or unsupervised.

The central nervous system sends sensory information and the activities that go with it all across the body [2]–[4]. Brain is most intricate organism in human body. It serves various roles and controls the operations of the body's other systems. The brain's frontal lobe aids in motor control, problem solving, and decision making. The parietal lobe regulates body posture. Memory and hearing are handled by the temporal lobe, whereas vision is handled by the occipital lobe. The cerebral cortex is a grey substance that surrounds the cerebrum and is made up of several neurons. The cerebellum regulates different voluntary movements in living animals equipped with nervous system. When brain cells grow abnormally and are not effectively managed, a brain tumor can form. A tumor is an abnormal collection of cells that is generated by uncontrolled cell division. It has been discovered that all tumor variations are not malignant. Brain tumors are the world's tenth largest cause of mortality. Cancer, in its most basic sense, refers to malignant tumors rather than benign ones. There are two categories of brain tumours: grades 1 and 2 (low) and grades 3 and 4 (high).

Computer-Aided Diagnosis (CAD) can be extremely beneficial in the investigation, prognosis, along with the remedy of brain tumors. A typical brain tumor CAD system includes three major phases: tumor ROI segmentation, feature extraction, and classification (based on the retrieved features) [5]. The most significant and time-consuming aspect of such a system is brain tumor segmentation, which may be done manually or automatically. The requirement of tracing ROIs is an evident restriction of such systems, which might pose a few issues. First of all, because of the varying nature of brain tumors greatly in shape, size, and location, tracing ROIs may be difficult and frequently not totally automated. This may result in severe segmentation mistakes that aggregate into subsequent phases, resulting in erroneous categorization. Second, tumor-surrounding tissues are thought to be distinct between tumor classifications. Third, relying entirely on ROI characteristics implies full ignorance of tumor location information, which might have a significant impact on categorization.

The aforementioned issues inspire us to offer an alternate technique for classifying brain tumor that fully eliminates the segmentation step. Brain tumour detection is critical in biological applications. The brain tumor grouping continue to help doctors in disease diagnosis. Throughout the classification process, many operations including as preprocessing, feature extraction, and classification are necessary. Preprocessing is a stage in image processing that happens before feature extraction to establish the location of an area or item. This technique

includes filtering, standardizing, and identifying things prior to the extraction stage. The method of obtaining essential numeric values from photographs in order to distinguish them is known as feature extraction.

Brain MRI image is mainly used to diagnose tumors as well as to mimic tumor growth. The data is generally employed in tumor detection and therapeutic methods. An MRI image contains more information than a CT or ultrasound image. An MRI scan can detect anomalies in brain tissue and offer extensive information on brain architecture. MRI may detect a variety of brain diseases, which include abnormalities like cyst and tumor. It can detect white and gray matter of brain. Tumor diagnosis at an early stage is crucial since tumors may be hazardous in many scenarios and, in the worst-case scenario, lead to death. As a result, tumor prediction utilizing automated algorithms may be of great help in tumor identification and is the most secure option.

Convolutional neural networks (CNNs) are a type of deep learning technique which is extensively used in image processing. It is based on basic activities of the human brain [6]. CNNs have several advantages over ordinary machine learning networks, which can be achieved by increasing the number of training data, leading in an efficient and resilient model [7]. CNN is used in image processing techniques such as MRI image segmentation, identification, and classification, together with brain cancer classification and detection. Therefore, we offer a fully automatic CNN-based MRI image segmentation along with classification system for three types of malignancies: meningioma, glioma, and pituitary tumors in this study.

The remainder of the paper is divided into the following subsections. Section II goes over the existing literature on brain MRI classification. Section III describes the convolutional neural network. Section IV elaborates a detailed survey on some popular deep learning based MRI classification techniques. Section V describes analysis of MRI images using CNN architecture. Section VI describes the proposed CNN methodology. Section VII elaborates on the experimental work and compares it to the current state-of-the-art CNN model. Section VIII describes the experimental results. Section IX describes the limitation of the existing CNN architecture. Section X discusses about the experimental results. Finally section XI concludes the research paper.

II. Literature Survey

Segmenting the region of interest from an item is one of the most complex and time-consuming processes, and segmenting the tumor from an MRI Brain image is a major one. Several current publications divide brain images into normal (tumorous) and pathological categories (non-tumorous). Al-Baderneh et al. [8] investigated the arrangement of brain MRI applying Artificial Neural Network as well as K-Nearest Neighbour (KNN) including textural characteristics utilizing 181 images of sick brains as well as 94 images of normal brains. The study [9] describes how to use feed-forward back-propagation to classify MRI vision as abnormal or normal. The particular algorithms are supervised (classes are known) and need feature retrieval before classification. Rajesh et al. [10] provide one such strategy, in which they conducted classification using a Feed Forward Neural Network with ternary layers, 50 nodes in the hidden layer, along with single output node. Provisional investigation can be found in [11] as well as Taie et al. [12] used Support Vector Machine (SVM) to accomplish classification.

Cutting-edge deep learning algorithms are being developed in tandem with these technologies. Many of these works do not employ brain imaging to determine if something is normal or pathological, but they were included since they were done on a variety of other sorts of distribution. Pereira et al. [13] employed CNN to identify gliomas in their article. Deep learning was utilized by Kamnitsas et al. [14] to classify ischemic stroke. The author [15] examined the Adaptive Network-based Fuzzy Inference Approach, a suggested technique for categorizing tumors into five classes (ANFIS). Another study used pre-trained AlexNet to categorize and segment tumors depending on Gray-Level Co-Occurrence Matrix (GLCM) features [16]. SVM [17], CNN [18], other studies include Recurrent Neural Network (RNN) [19], AlexNet transfer learning network of CNN [20], VGG-16, Inception V3 and ResNet50 [21], along with CNN quartet technique.

The authors suggested a strategy for glioma classification that merged SVM and KNN in [22]. The accuracy for multi-classification is 85%, but the accuracy for binary classification is 88%. Ertosun and Rubin [24] advocated using CNN to differentiate between low along with high grade gliomas as well as their grades. They achieved 71% as well as 96% accuracy, respectively. Using axial brain tumor pictures, Paul et al. [23] trained and developed two unique classification algorithms (a fully connected CNN). The CNN architecture's accuracy was 91.43%, with two convolutional layers followed by two fully linked layers. M Malathi, P Sinthia, and colleagues [25] demonstrated completely automatic brain tumour segmentation using a convolutional neural network. Brain tumours and gliomas were the most common and lethal, with little life suspense on its highest level. Manual segmentation was a time-consuming task in medical practise, and its execution was highly dependent on the operator's experience. J. Seetha and S. Selvakumar Raja et al. [26] demonstrated that the massive amount of data generated by MRI impedes manual classification of tumour vs non-tumor at an exacting time. However, it has a few limitations (i.e. precise quantitative measurements were given for a restricted number of images). The classification of brain tumours using convolutional neural networks is described in this paper.

Vipin Y. Borole, Sunil S. Nimbhore, and Dr. Seema S. Kawthekar discuss brain tumours [27]. Because of the structure of the brain, brain tumour recognition is a difficult task for MRI images. A brain tumour is an unusual development of cerebrum cells. X-ray images provide better contrast of various delicate tissues of the human body. X-ray images outperform CT, Ultrasound, and X-beam images. In this, various preprocessing, post-processing, and strategies such as (Filtering, difference improvement, Edge recognition) and post-processing systems such as (Histogram, Threshold, Segmentation, Morphological operation) are accessible in MATLAB for the location of brain tumour images via image handling (IP) apparatus (MRI-Images). Gooya et al. [28] presented GLISTR, a method for segmenting gliomas in multi-modal MR images by registering the images to a probabilistic atlas of healthy individuals. The incorporation of the tumour

growth model into the anatomy of the patient brain was the major contribution. Based on histogram analysis of temporal Magnetic Resonance Image (MRI) data, Manikis et al. [29] proposed a novel framework for assessing tumour changes. The proposed method detects tumour distribution and quantitatively models its growth or shrinkage, potentially assisting clinicians in objectively assessing subtle changes during treatment.

Bauer et al. [30] developed a novel method for converting a healthy brain atlas to MR images of tumour patients. They presented a new method for adapting a general brain atlas to an individual tumour patient image that uses sophisticated models of bio-physio mechanical tumour growth. Roy et al. [31] proposed an investigation into automated brain tumour detection and segmentation from brain MRI. Brain tumour segmentation was an important step in extracting information from complex MRI brain images. Sindhushree K.S et al. [32] created a brain tumour segmentation method and validated it using two-dimensional MRI data. In addition, detected tumours are represented in three dimensions. To detect tumour, high pass filtering, histogram equalisation, thresholding, morphological operations, and segmentation using connected component labelling were used. The extracted two-dimensional tumour images were reconstructed into three-dimensional volumetric data, and the tumour volume was calculated.

Ertosun and Rubin [24] proposed using CNN to distinguish between low and high grade gliomas and their grades. They achieved 71% and 96% accuracy, respectively. Krol et al. [33] used axial brain tumour images to train and develop two distinct classification approaches (a fully connected CNN). The accuracy of the CNN architecture, which consisted of two convolutional layers followed by two fully connected layers, was 91.43%. In the next section, we will go through the various methods for classifying MRI as normal or abnormal.

III. Convolutional Neural Networks

Convolution is a convolution layer approach placed on a linear algebra operation which helps in multiplying the filter in the image [34]. CNN is a neural network that analyses information by using a grid topology. The convolution layer, is used as the first panel. It changes the input data without altering initial information. Another frequent sort of layer is the pooling layer, which is used to compute the maximum or average value of the image's pixel coordinates. By generating a feature map, CNN can learn complex features.

A. Brain Imaging Modalities

To assess the brain structure, four basic technologies (CT, PET, DWI, and MRI) are commonly employed for brain malignancies.

1) Computed Tomography (CT): A CT scan is a diagnostic imaging test that produces images of the internal body using X-ray technology. CT scans are utilized to evaluate and diagnose brain abnormalities, they are also used to assist various surgical operations. It creates a 3D image of soft tissues along with bones using X-rays and a computer. CT is a non-invasive, painless technique for your healthcare professional to diagnose issues. CT scans are commonly performed with and without contrast agents to help the radiologist detect any abnormalities.

2) Position Emission Tomography (PET): PET is used to evaluate brain metabolism as well as the distribution of radio labeled chemical agents in the brain. PET detects emissions from metabolically active compounds that have been radioactively labelled and circulated throughout the body. The brain emission data PET scans are computer-processed to provide multidimensional pictures of chemical distribution throughout the brain. PET is a sort of functional imaging which can detect metabolic anomalies such as glucose metabolism, blood flow, oxygen consumption, amino acid metabolism and liquid synthesis. These measures represent the amount of brain activity in distinct brain areas and help us to understand more about how the brain functions. When they initially became available, PET scans outperformed all other metabolic imaging modalities in terms of resolution and completion time (as low as 30 seconds).

3) Diffused Weighted Image (DWI): Diffusion weighted imaging (DWI) is a technique for producing signal contrast based on Brownian motion changes. DWI is a method used to evaluate the human body's molecular function and microarchitecture. DWI is a critical component of today's cutting-edge magnetic resonance imaging and is widely employed in neuro-imaging and cancer research. DWI is a continuously changing technological field, with new applications emerging on a regular basis.

4) Magnetic Resonance Imaging (MRI): MRI is one of the most popular imaging procedures utilized before and after surgery, with the goal of giving critical information for the treatment plan. In the medical industry, MRI is commonly used to identify and see elements in the body's internal structure. It is used to identify differences in biological tissues and is significantly superior to computed tomography (CT). Strong magnets are used in magnetic resonance imaging (MRI) scanners to polarise and excite hydrogen nuclei (one protons) in human tissue, creating a measurable signal that is spatially recorded and translated into body images. The proper interpretation of brain MRI images is vital for gathering important information that can aid in the early identification and diagnosis of illnesses.

B. Contributions

Convolutional Neural Networks (CNNs) have shown to be extremely fruitful in diagnosing a wide range of disorders and are commonly utilized in bio-medical image analysis. Those networks are particularly useful in detecting, classifying, and segmenting brain cancers in MRI datasets. Our approach's primary goals are as follows:

- Using deep learning and convolutional neural networks to detect brain cancers in MRI datasets.
- Experiment findings have shown that enlarging a dataset utilizing rotation, flipping, and translation approaches is quite beneficial for training the VGG architecture.

IV. A Detailed Survey on some Popular Deep Learning based MRI Classification Techniques

A. MobileNet V2

MobileNet-V2 is a 53-layer deep convolutional neural network. It enables real-time categorization in devices with

little computing power, such as smart phones. MobileNetV2 has an inverted residual architecture, with narrow bottleneck layers functioning as the residual blocks' input and output. It also uses lightweight convolutions to filter features in the expansion layer. Finally, nonlinearities in thin layers are eliminated. MobileNetV2 enhances the up-to-date execution of mobile models on a variety of tasks along with benchmarks, as well as over a wide range of model sizes. It is a powerful component for obtaining the object recognition and segmentation. MobileNetV2 is a feature extractor with tremendous capability for object segmentation and detection.

Advantages

- Network size has been reduced to 17MB.
- The number of parameters has been reduced to 4.2 million.
- They are faster in performance and excellent for mobile apps.
- A convolutional neural network with a low latency.
- MobileNets employ depth-wise separable convolutions in a simplified design.
- MobileNet employs two simple global hyperparameters to efficiently trade off accuracy for latency.
- MobileNet might be utilized for item identification, fine-grain categorization, face recognition, large-scale geolocation, and other applications.

B. ResNet101

The residual block is the fundamental basic element of ResNet101. As we proceed further into the network with a large number of layers, the computation gets increasingly complicated. These layers are built on top of one another, with each layer attempting to learn an underlying mapping of the desired function. We try to fit a residual mapping instead of these pieces. Another benefit of this extremely deep architecture is that it enables for up to 150 layers of this, which we then stack on a regular basis. We additionally double the number of filters and use stride two to spatially down sample. Finally, only layer 1000 was entirely linked to output classes. The fundamental loss of the present network is that due to the enormous number of parameters, assessing it is fairly expensive [35]. The ResNet101 focuses largely on treating the second non-linearity as an identity mapping, which implies that the result of the addition operation between the identity mapping and the residual mapping should be sent immediately to the next block for processing. Batch Normalization is at the heart of ResNet101. Batch Normalization modifies the input layer to improve network performance. The problem of covariate shift is solved. The Identity Connection is used by ResNet101 to assist avoid the network from experiencing the vanishing gradient problem. Deep Residual Network improves network speed by leveraging bottleneck residual block design.

Advantages

- Networks with several layers (even thousands) may be trained simply without increasing the training error percentages.
- ResNets can help solve the vanishing gradient problem by using identity mapping.

C. DenseNet121

DenseNet121 is a novel category of convolutional neural network in which all previous layers are linked to the current layer. A DenseNet121 is a sort of convolutional neural network that connects all levels directly by using dense connections between layers through Dense blocks. A deep DenseNet121 is defined as a collection of DenseNets (referred to as dense blocks) with extra convolutional and pooling operations performed between each dense block. DenseNet121 connects layers together using dense blocks [36]. DenseNet connects each layer to every other layer. This is incredibly effective.

Advantages

- They address the problem of disappearing gradients.
- They enhance feature dissemination.
- They promote feature reuse; and
- They minimize the number of parameters greatly.

V. Analysis of MRI Images using CNN Architecture

Classification is important because it arranges images into distinct groups. It is the first step in diagnosing any disease by forecasting an area or region having anomalies. The CNN model has several layers, including the convolution layer, pooling layer, flatten layer, dropout layer, and dense layer. In addition to the layers used in the CNN process, this study includes an activation function based on rule activation. An image in the shape of a number that interweaves the first convolution, with a resolution of 240x240 pixels. Kernels with a size of 3x3 and a thickness of three are used in accordance with the channel of the image data and filters. The model will perform the activation and data pooling functions after receiving the results of the operation. The Pooling layer process reduces the size of the feature map. The convolution process produces a feature map, which is then used for subsequent convolution processes. The next step is to flatten the feature map into vector form in order to perform a fully-connected layer process to produce image classification. This section briefly examines three alternative deep learning architectures (DenseNet121, MobileNet V2, and ResNet101) in addition to the recommended approach. Because of its successful performance in image classification that automatically finds key parts, CNN was employed to carry out the recommended classification strategy for brain MRI images. Fluid Attenuated Inversion Recovery (FLAIR) of MRI is the imaging method used here. It looks like a T2 picture but has a relaxation time (TR) along with longer echo (TE). The present sequencing is the disease perceptive as well as greatly simplifies the distinguishing CSF from an aberration.

VI. Proposed Model

A. MobileNet V2 Model

MobileNet-V2 is a fully convolutional network designed for mobile devices. It has an inverted residual framework,

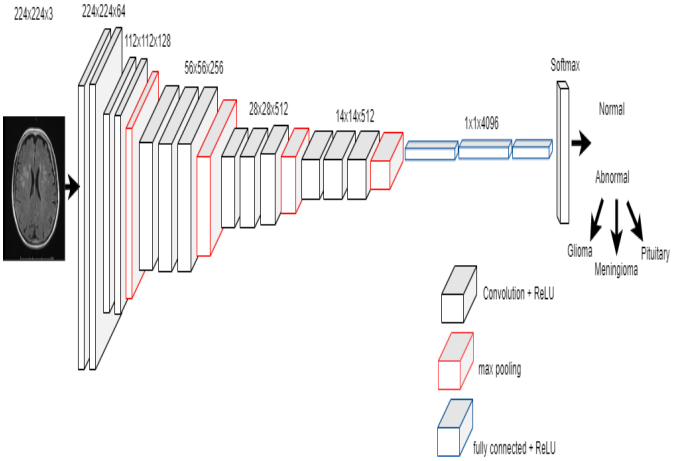

Fig. 1. MobileNet-V2 Model.

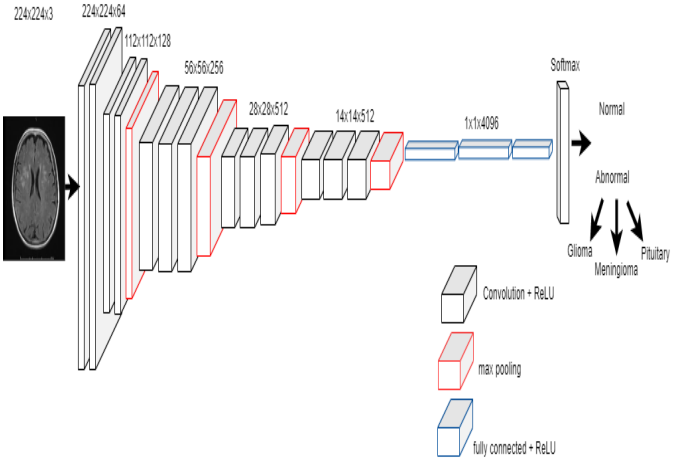

Fig. 2. ResNet Model.

along the congestion layers associated with residual connections. As a source of nonlinearity, the intermediate extension layer filters features with lightweight depth-wise convolutions. The original and improved images come in a variety of range. The first phase is via eliminating the noise from an image by using preprocessing, via median filtering. After that, the images are shrunk to a precise magnitude of 124x124x3 to ensure that they are not at all tiny; that is done to preserve the proportion along with the assists in improved training assuming that the sizes are just the same. The magnitude of 124 was selected since it is the fundamental size of accessible image. The images continue to turn into gray scale for easier understanding of characteristics. The particular images are then transferred to the convolutional layer, the most essential part of a CNN. Fig. 1 shows how the stride varies in each convolutional layer. The MobileNetV2 model has a total parameter count of 2,263,108 and consists of a first fully convolutional layer with 32 filters, followed by 17 residual bottleneck layers and the activation function Relu. It achieves promising accuracy results while using less computing memory and resources. Furthermore, it transforms them into a high speed network for image processing jobs by using dropout, dense followed by softmax activation function. MobileNetV2 is a lightweight convolutional neural network utilized in synchronous functions. First, it has 2,228,996 trainable parameters than classic convolution, which minimizes computing expenses, along with 34,112 parameters are used as non-trainable parameters.

B. ResNet101

Using ImageNet data, ResNet101 took first state in the ILSVRC 2015 classification test. Because the pre-trained representation is used straight-forwardly for image categorization, transfer learning is adaptive. The images are trimmed such that just the brain area is visible. Preprocessing is the initial stage in removing noise from a image. After median filtering, the images are shrunk to an exact size of 124x124x3 to ensure that they are not too small; this preserves the ratio and aids in better training if the sizes are all the same. Because it is the least accessible, the image size of 124 was chosen. For improved learning of characteristics, the images are turned to gray scale. These images are subsequently transmitted to the convolutional layer, which is the most crucial aspect of a CNN. Fig. 2 shows how stride varies in each convolutional layer along with pooling layer. The network can accept input images with height and width multiples of 32 and channel width of three. For the purpose of clarity, we'll assume the input size is 224 × 224 x 3. The kernels utilised to conduct the convolution operation in all three levels of the stage 1 block are 64, 64, and 128 correspondingly. Because the convolution operation in the Residual Block is conducted with stride 2, the size of the input is decreased to half in terms of height and width, while the channel width is doubled. As we advance through the stages, the channel width doubles and the input size is cut in half. Each pooling method is repeated for five times. Flattening is an important layer following pooling since we need to turn the whole matrix representing the input images into a single column vector, which is required for processing. The data is subsequently put into the Neural Network for processing. The model is trained and updated using the dataset under consideration for our study to solve two-class problems with outputs of abnormal (class 0) as well as normal (class 1). The ResNet50 model has a total parameter count of 42,666,372 and consists of a first fully convolutional layer with 32 filters, followed by 15 residual bottleneck layers and the activation function Relu. It achieves promising accuracy results while using less computing memory and resources. Furthermore, it transforms them into a high speed network for image processing jobs by using dropout, dense followed by softmax activation function. First, it has 42,561,028 trainable parameters than classic convolution, which minimizes computing expenses, along with 105,344 parameters are used as non-trainable parameters.

C. DenseNet121

The first step is to use preprocessing to eliminate noise from a image. It is accomplished by the use of median filtering. The median filter is used to eliminate outliers from a picture while preserving the image's information. The photos are scaled to an exact size of 124x124x3 after median filtering to ensure that they are not too tiny; this retains the ratio and assists in better training if the sizes are all the same. The image size of 124 was chosen since it is the least accessible.

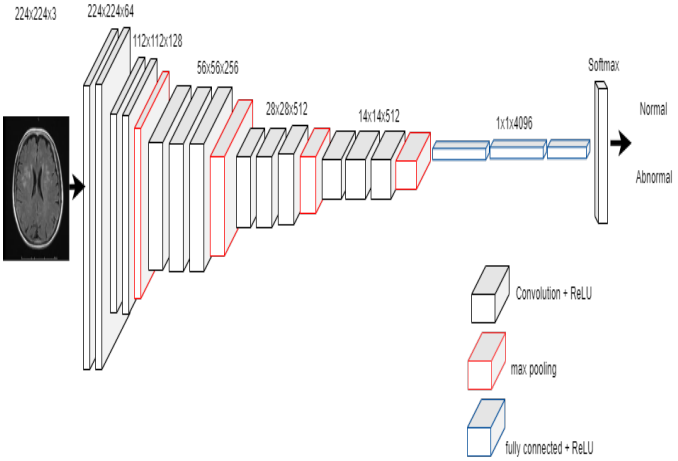

Fig. 3. DenseNet Model.

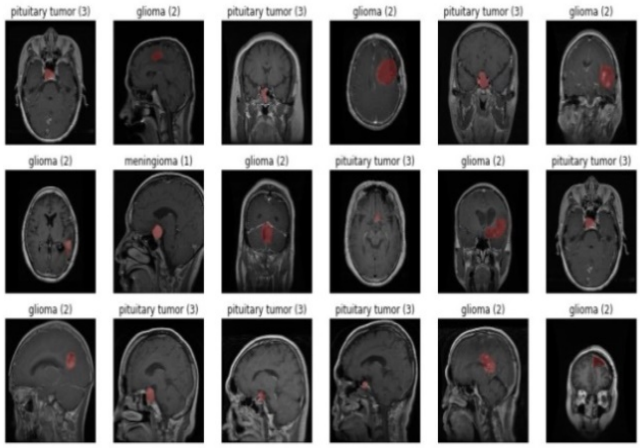

Fig. 4. Dataset of Brain Tumor.

For improved feature learning, the images are transformed to gray scale. These images are subsequently sent to the convolutional layer, which is the most critical aspect of a CNN. Figure 3 shows how the stride varies in each convolutional layer. DenseNet121 employs a first fully convolutional layer with 57 filters, followed by 119 residual bottleneck layers and activation function maximum pooling with 7,047,504 total parameters. The network may accept input images with height, width multiples of 32, and channel width of three. For the sake of clarity, we will take the input size to be 224 × 224 x 3. The kernels utilised to execute the convolution operation in all three levels of the block of stage 1 are 64, 64, and 128 correspondingly. Because the convolution operation in the Residual Block is conducted with stride 2, the size of the input will be decreased to half in terms of height and breadth, but the channel width will be doubled. As we move through the stages, the channel width doubles and the size of the input is cut in half. Instead of using the Gradient descent (GD) technique, the Adam optimizer was used, which maintains a consistent learning rate for each weight in a network. Dropout, a regularizer, is used in our technique in completely linked layers. For this reason, a rate of 0.5 is specified. As a loss function, the binary cross-entropy loss function (log loss) was used. Finally, ReLU is used in conjunction with the Adam optimizer for classification, where 0.5 is classified as [1 0] (abnormal) and anything else as [0 1] (normal). The DenseNet model has a total parameter count of 7,041,604 and consists of a first fully convolutional layer with 32 filters, followed by 15 residual bottleneck layers and the activation function Relu. It achieves promising accuracy results while using less computing memory and resources. Furthermore, it transforms them into a high speed network for image processing jobs by using dropout, dense followed by softmax activation function. First, it has 6,957,956 trainable parameters than classic convolution, which minimizes computing expenses, along with 83,648 parameters are used as non-trainable parameters.

VII. Experiments and Analysis of Results

The information came from the open-source Kaggle database. The collection contained X-ray photos of healthy and brain tumour patients. To extract the characteristics, a CNN model is used. Four Conv2D layers, three Maxpooling2D levels, one flatten layer, two dense layers, and a ReLu activation function comprise the model. The ReLU function is used to activate the last thick layer. The primary goal of this research is to evaluate the accuracy of the planned model to that of the pretrained model. The final layers are fully adjustable, with options such as Average Pooling, Flatten, Dense, and Dropout.

A. Dataset Used

Magnetic Resonance Imaging is the most effective tool for detecting brain cancers (MRI). The scans yield massive quantities of data pictures, which the radiologist examines. We propose a classification model in this paper that would allow us to take MRI pictures of the patient as input and calculate whether or not a tumour exists in the brain as output. The dataset of the proposed framework has been taken from the kaggle repository as shown in Fig. 4. The dataset contains 826 brain MRI images of glioma tumor, 822 images of meningioma tumor, 847 images of pituitary tumor, and 395 images with no tumor. As a result, there are 2890 images in total. 80% of the dataset has been used for training where as 20% for testing purposes. X-ray images of both healthy and brain tumor patients were included in the collection. The models learn to recognize images based on the properties extracted from the provided images. To eliminate noise, the dataset was gathered locally and pre-processed with an adaptive histogram equalizer.

B. Tools Used

To carry out the implementation, the Python programming language is employed. Keras and TensorFlow are the libraries utilized. Several Python-based packages are studied in this study to implement our techniques.

C. Preprocessing

The modified curvature diffusion equation (MCDE) is used to normalize image intensity as additional step in the preprocessing phase. The Wiener filter is used in medical imaging to increase local and spatial information. When the noise level is excessive, it is difficult to recover the edge of

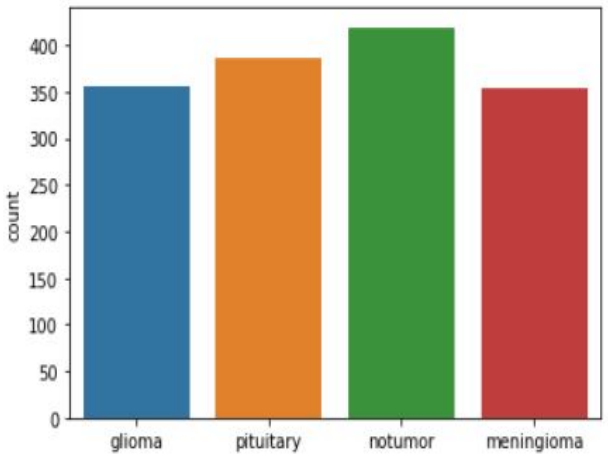

Fig. 5. Testing Simulation Result of Dataset.

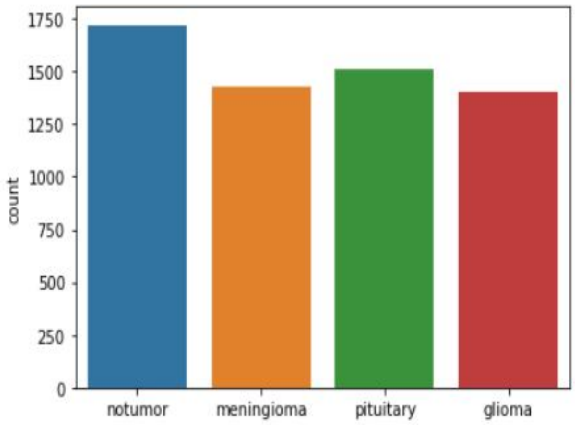

Fig. 6. Training Simulation Result of Dataset.

an image. Because images have distinct variations in intensity, contrast, and size, pre-processing is used to provide smooth training [12]. The wrapping and cropping method will be applied to the input image in the first pre-process. The input image is verified against the edge of the major object in the image during wrapping. Cropping occurs when the biggest edge of an image is set so that the item in the image stays intact. Because the picture sizes in the collection differ, resize the image to (240x240x3) = (image width x image height x number of channels). To aid in learning, normalise pixel values to the 0-1 range. The next step is to make an array out of each photograph in the collection. The image is used as a preprocessed input by MobileNetV2, DenseNet, and ResNet50. Coding is the final stage. The tagged data is converted into a numerical label, which may be understood and evaluated. The dataset is then separated into three sections: 20% for validation, 70% for training, and the remaining for testing.

D. Performance Metrics

Researchers evaluate many performance indicators in classification, with accuracy being the most commonly used performance parameter. Accuracy, precision, F1 Score, and support are the parameters used to validate our results.

VIII. Experimental Results

To categorize the images as normal or abnormal, MobileNet V2, DenseNet121, and ResNet101 are used. The implementation is separated into two parts: general categorization into normal or abnormal brain tumors and specific classification into different categorises of the brain tumors. There are two approaches: k fold cross validation with k fold = 5 as well as 8 (arbitrary values), along with the generalisation strategy, which does not use training phase data in the testing phase. Both training as well as testing evidence of the used dataset are represented in Table I.

The graphical representation of result of the testing simulation is shown in Fig. 5 and the result of the training simulation is shown in Fig. 6.

	precision	recall	f1-score	support
0	0.93	0.99	0.96	356
1	0.97	0.92	0.94	353
2	0.99	1.00	0.99	419
3	1.00	0.97	0.99	387
accuracy			0.97	1515
macro avg	0.97	0.97	0.97	1515
weighted avg	0.97	0.97	0.97	1515

Fig. 7. Classification Report of MobileNet-V2 Model.

A. Results and Analysis

In MobileNetV2, total parameters 2,263,108 are used. Out of which, 2,228,996 are used as a training parameters and 34,112 are used as a non-training parameters.

Fig. 7 shows the classification results for parameters such as precision, recall, f1-score as well as support for four classes of dataset used along with macro-average accuracy of 97% and weighted-average accuracy of 97%.

Fig. 8 shows the confusion matrix for the four classes of tumor dataset in MobileNet-V2 Model, which shows exponential value as 3.5e+02, that means the accurate values is 350 in decimal for glioma tumor, exponential value as 3.2e+02, that means the accurate values is 320 in decimal for meningioma tumor, exponential value as 4.2e+02, that means the accurate values is 420 in decimal for normal patients and exponential value as 3.8e+02, that means the accurate values is 380 in decimal for pituitary tumor patients.

Fig. 9 shows the graphical representation of the training and validation accuracy/loss for the MobileNet-V2 model. The testing accuracy and loss is almost constant for number of

TABLE I. TESTING-TRAINING SIMULATION RESULT OF THE DATASET

Types of tumor	Testing Simulation result	Training Simulation Result
Glioma tumor	350	1400
Pituitary tumor	375	1500
No tumor	425	1700
meningioma tumor	340	1400

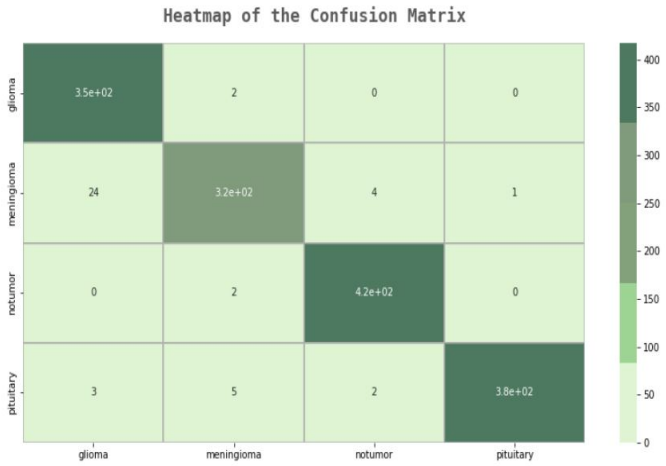

Fig. 8. Confusion Matrix of MobileNet-V2 Model.

	precision	recall	f1-score	support
0	1.00	0.99	0.99	356
1	0.98	0.99	0.99	353
2	1.00	0.99	1.00	419
3	0.99	1.00	0.99	387
accuracy			0.99	1515
macro avg	0.99	0.99	0.99	1515
weighted avg	0.99	0.99	0.99	1515

Fig. 10. Classification Report of DenseNet Model.

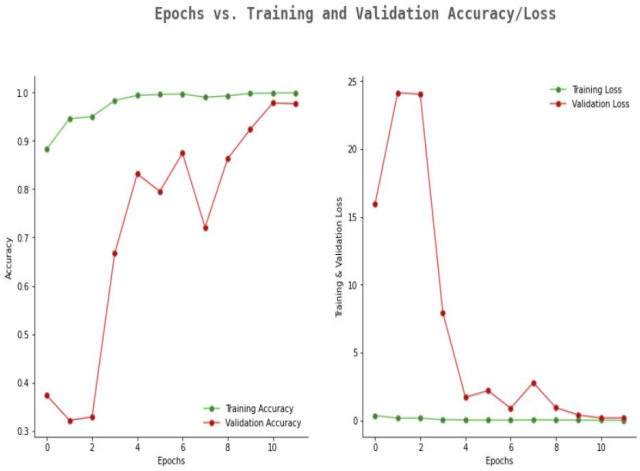

Fig. 9. Training and Validation Accuracy/Loss of MobileNet-V2 Model.

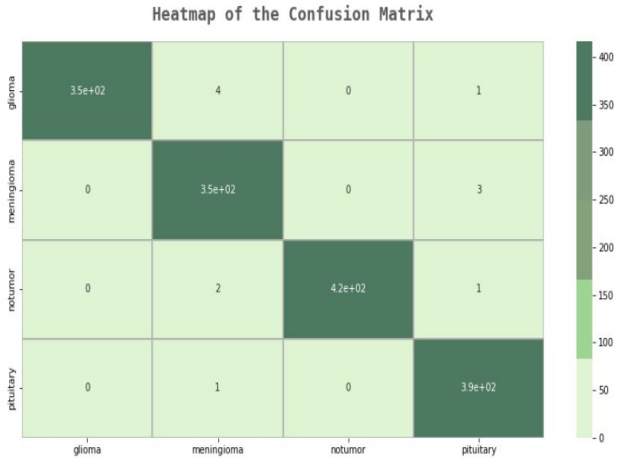

Fig. 11. Confusion Matrix of DenseNet Model.

epochs, whereas the validation accuracy and loss is varying greatly for number of epochs.

In DenseNet121, total parameters 7,047,504 are used. From which, 6,966,026 parameters are used as a training and 81478 are used as a non-training parameters.

Fig. 10 shows the classification results for parameters such as precision, recall, f1-score along with support of four classes of dataset used as well as macro-average accuracy of 99% and weighted-average accuracy of 99%.

Fig. 11 shows the confusion matrix with the measures of 3.5e+02 in exponential form, that means the accurate values is 350 in decimal for glioma tumor, the exponential value as 3.5e+02, that means the accurate values is 350 in decimal form for meningioma tumor, measures of 4.2e+02 in exponential form, that means the accurate value is 420 in decimal form for no tumor and the exponential value as 3.9e+02, that means the accurate values in decimal form is 390 for pituitary tumor patients dataset in DenseNet Model.

Fig. 12 shows the graphical representation of the training and validation accuracy/loss for the DenseNet121 model. The testing accuracy and loss is almost constant after certain number of epochs, whereas the validation accuracy and loss is varying greatly at the beginning for number of epochs but after certain number of epochs it comes to a constant value.

Total parameters used for ResNet101 model are

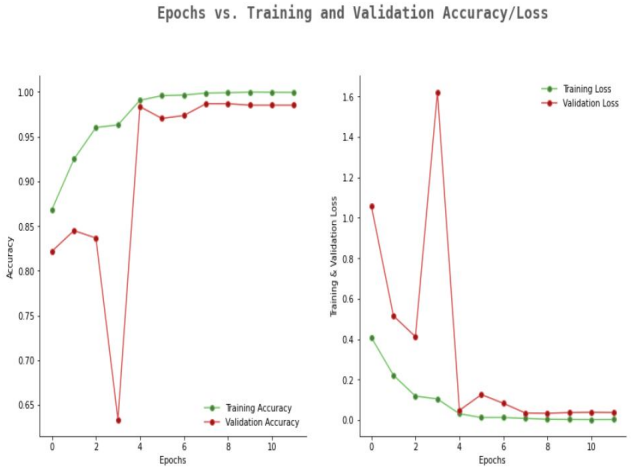

Fig. 12. Training and Validation Accuracy/Loss of DenseNet Model.

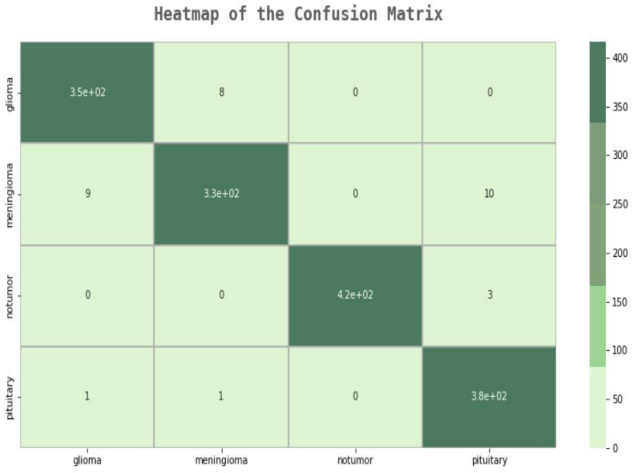

Fig. 14. Confusion Matrix of ResNet101 Model.

	precision	recall	f1-score	support
0	0.97	0.98	0.97	356
1	0.97	0.95	0.96	353
2	1.00	0.99	1.00	419
3	0.97	0.99	0.98	387
accuracy			0.98	1515
macro avg	0.98	0.98	0.98	1515
weighted avg	0.98	0.98	0.98	1515

Fig. 13. Classification Report of ResNet101 Model.

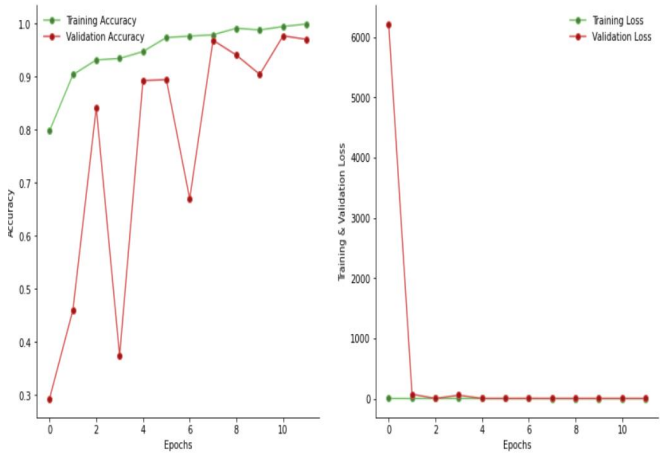

Fig. 15. Training and Validation Accuracy/Loss of ResNet101 Model.

21,963,424. Out of which, 21,961,408 are used as a training parameters and 2,016 are used as a non-training parameters.

Fig. 13 shows the classification results for parameters such as precision, recall, f1-score as well as support of four classes of dataset used along with macro-average accuracy of 98% as well as weighted-average accuracy of 98%.

Fig. 14 shows the confusion matrix for the four classes of tumor dataset, which shows 3.5e+02 as exponential value, that means the accurate values is 350 in decimal for glioma tumor, 3.3e+02 as exponential value, that means the accurate values is 330 in decimal form for meningioma tumor, the exponential value as 4.2e+02, that means the accurate value is 420 in decimal for no tumor and the exponential value as 3.8e+02, that means the accurate value is 380 in decimal for pituitary tumor in ResNet Model.

Fig. 15 depicts a graphical depiction of the ResNet101 model's training and validation accuracy/loss. The testing accuracy and loss are practically constant for the number of epochs, but the validation accuracy varies substantially with the number of epochs, but the validation loss is constant.

IX. Limitations of Existing Machine Learning Methods

The following are the primary difficulties in detecting brain tumors:

- It is still difficult to detect a little quantity of tumour since it might be mistaken for a normal region.
- Some existing techniques are effective in one tumour site but not in another (enhanced or non-enhanced), and vice versa.

X. Discussion

The Table II displays the comparison of loss along with accuracy values for test parameters of different machine learning methods. The following parameters such as precision, recall, F1 score and accuracy have been used to assess the prediction results. Obtained values of precision, recall, F1 score as well as support for classification of ML models are represented

TABLE II. COMPARISON OF LOSS AND ACCURACY VALUES FOR TEST PARAMETERS OF DIFFERENT MACHINE LEARNING METHODS

Machine Learning Methods	Test Loss	Test Accuracy
MobileNet-V2	3.8652	0.30735
DenseNet121	0.25539	0.893838
ResNet101	0.082731	0.971789

in Table III. MobileNet-V2 models are the least suited for the image classification of brain tumors, as the accuracy for both macro-average and weighted-average is 97%. It can be seen that DenseNet model shows best results, which shows the accuracy for both macro-average and weighted-average is 99% due to its improved generalization and embedded ensemble learning feature. Our experimental performance proves the highest for our proposed CNN model with an accuracy of 92% which is more than all other models trained.

Following a thorough examination of existing state-of-the-art approaches, the following challenges have been identified:

- A brain tumor grows rapidly in size. As a consequences, early tumor diagnosis is an extremely important job.
- MRI pictures are inaccurately classified due to magnetic field changes in the coil.
- Another tough procedure is the structured and best feature extraction and selection.

XI. CONCLUSION

Convolutional neural networks are still a hot topic in the field of automated tumor segmentation. It is critical for radiologists to understand convolutional neural networks in order to be prepared to use these technologies in clinical practice in the future. A thorough examination of several CNN designs was conducted along with their limitations when faced with a small dataset. One of the most significant fields of medical imaging is the hunt for a treatment for various forms of brain tumours. To avoid overfitting, this article employs a data augmentation approach prior to classification. To reach a conclusion, we examined three machine learning approaches: MobileNet-V2, DenseNet121, and ResNet101. However, this study demonstrates the significance of supervised learning approaches in the development of CAD systems to reduce the burden on radiologists. A future investigation could include collecting larger brain MR images to generalise the classifier systems. T2-weighted contrast-weighted MRI images were used in this study. The fundamental purpose of this project is to develop a high-accuracy, high-performance, and low-complexity automated brain tumour classification system. As the loss for test parameters is very high for MobileNe-V2 i.e. 3.8652 as compared to DenseNet121 i.e. 0.25539 and ResNet101 i.e. 0.082731, due to lot of errors, so this MobileNet V2 model is going to be modified in our future work.

REFERENCES

[1] Devi, S., Sahoo, M. N., Muhammad, K., Ding, W., & Bakshi, S. (2019). Hiding medical information in brain MR images without affecting accuracy of classifying pathological brain. Future Generation Computer Systems, 99, 235-246.

[2] Park, J. G., & Lee, C. (2009). Skull stripping based on region growing for magnetic resonance brain images. NeuroImage, 47(4), 1394-1407.

[3] Khan, M. A., Lali, I. U., Rehman, A., Ishaq, M., Sharif, M., Saba, T., ... & Akram, T. (2019). Brain tumor detection and classification: A framework of marker-based watershed algorithm and multilevel priority features selection. Microscopy research and technique, 82(6), 909-922.

[4] Raza, M., Sharif, M., Yasmin, M., Masood, S., & Mohsin, S. (2012). Brain image representation and rendering: A survey. Research Journal of Applied Sciences, Engineering and Technology, 4(18), 3274-3282.

[5] Watson, C., Kirkcaldie, M., & Paxinos, G. (2010). The brain: an introduction to functional neuroanatomy. Academic Press.

[6] Matsugu, M., Mori, K., Mitari, Y., & Kaneda, Y. (2003). Subject independent facial expression recognition with robust face detection using a convolutional neural network. Neural Networks, 16(5-6), 555-559.

[7] Litjens, G., Kooi, T., Bejnordi, B. E., Setio, A. A. A., Ciompi, F., Ghafoorian, M., ... & Sánchez, C. I. (2017). A survey on deep learning in medical image analysis. Medical image analysis, 42, 60-88.

[8] Al-Badarneh, A., Najadat, H., & Alraziqi, A. M. (2012, August). A classifier to detect tumor disease in MRI brain images. In 2012 IEEE/ACM International Conference on Advances in Social Networks Analysis and Mining (pp. 784-787). IEEE.

[9] Mohsen, H., El-Dahshan, E. S. A., & Salem, A. B. M. (2012, May). A machine learning technique for MRI brain images. In 2012 8th International Conference on Informatics and Systems (INFOS) (pp. BIO-161). IEEE.

[10] Rajesh, T., & Malar, R. S. M. (2013, July). Rough set theory and feed forward neural network based brain tumor detection in magnetic resonance images. In International Conference on Advanced Nanomaterials & Emerging Engineering Technologies (pp. 240-244). IEEE.

[11] Balasubramanian, C., & Sudha, B. (2014). Comparative study of de-noising, segmentation, feature extraction, classification techniques for medical images. Int. J. Innov. Res. Sci. Eng. Technol, 3(3), 1194-1200.

[12] Taie, S. A., & Ghonaim, W. (2017, March). CSO-based algorithm with support vector machine for brain tumor's disease diagnosis. In 2017 IEEE International Conference on Pervasive Computing and Communications Workshops (PerCom Workshops) (pp. 183-187). IEEE.

[13] Pereira, S., Pinto, A., Alves, V., & Silva, C. A. (2016). Brain tumor segmentation using convolutional neural networks in MRI images. IEEE transactions on medical imaging, 35(5), 1240-1251.

[14] Kamnitsas, K., Ledig, C., Newcombe, V. F., Simpson, J. P., Kane, A. D., Menon, D. K., ... & Glocker, B. (2017). Efficient multi-scale 3D CNN with fully connected CRF for accurate brain lesion segmentation. Medical image analysis, 36, 61-78.

[15] Roy, S., & Bandyopadhyay, S. K. (2018). Brain tumor classification and performance analysis. Int. J. Eng. Sci, 8, 18541-18545.

[16] Krishnammal, P. M., & Raja, S. S. (2019, April). Convolutional neural network based image classification and detection of abnormalities in mri brain images. In 2019 International Conference on Communication and Signal Processing (ICCSP) (pp. 0548-0553). IEEE.

[17] Hamid, M. A., & Khan, N. A. (2020). Investigation and classification of MRI brain tumors using feature extraction technique. Journal of Medical and Biological Engineering, 40(2), 307-317.

TABLE III. CAMPARATIVE ANALYSIS OF CLASSIFICATION METRICS ON THREE DIFFERENT DEEP LEARNING TECHNIQUES

Machine Learning Methods	Types of tumor	Precision	Recall	F1-Score	Support
MobileNet-V2	Glioma tumor	0.93	0.99	0.96	356
	Meningioma Tumor	0.97	0.92	0.94	353
	No Tumor	0.99	1.00	0.99	419
	Pituitary Tumor	1.00	0.97	0.99	387
DenseNet121	Glioma tumor	1.00	0.99	0.99	356
	Meningioma Tumor	0.98	0.99	0.99	353
	No Tumor	1.00	0.99	1.00	419
	Pituitary Tumor	0.99	1.00	0.99	387
ResNet101	Glioma tumor	0.97	0.98	0.97	356
	Meningioma Tumor	0.97	0.95	0.96	353
	No Tumor	1.00	0.99	1.00	419
	Pituitary Tumor	0.97	0.99	0.98	387

[18] Hanwat, S., & Jayaraman, C. (2019). Convolutional neural network for brain tumor analysis using MRI images. Int. J. Eng. Technol, 11, 67-77.

[19] Kalaiselvi, K., Karthikeyan, C., Shenbaga Devi, M., & Kalpana, C. (2020). Improved Classification of Brain Tumor in MR Images using RNN Classification Framework. Int. J. Innov. Technol. Explor. Eng.(IJITEE), 9, 1098-1101.

[20] Wahlang, I., Maji, A. K., Saha, G., Chakrabarti, P., Jasinski, M., Leonowicz, Z., & Jasinska, E. (2022). Brain Magnetic Resonance Imaging Classification Using Deep Learning Architectures with Gender and Age. Sensors, 22(5), 1766.

[21] Khan, H. A., Jue, W., Mushtaq, M., & Mushtaq, M. U. (2020). Brain tumor classification in MRI image using convolutional neural network. Math. Biosci. Eng, 17(5), 6203-6216.

[22] Zacharaki, E. I., Wang, S., Chawla, S., Soo Yoo, D., Wolf, R., Melhem, E. R., & Davatzikos, C. (2009). Classification of brain tumor type and grade using MRI texture and shape in a machine learning scheme. Magnetic Resonance in Medicine: An Official Journal of the International Society for Magnetic Resonance in Medicine, 62(6), 1609-1618.

[23] Paul, J. S., Plassard, A. J., Landman, B. A., & Fabbri, D. (2017, March). Deep learning for brain tumor classification. In Medical Imaging 2017: Biomedical Applications in Molecular, Structural, and Functional Imaging (Vol. 10137, pp. 253-268). SPIE.

[24] Ertosun, M. G., & Rubin, D. L. (2015). Automated grading of gliomas using deep learning in digital pathology images: a modular approach with ensemble of convolutional neural networks. In AMIA annual symposium proceedings (Vol. 2015, p. 1899). American Medical Informatics Association.

[25] Malathi, M., & Sinthia, P. (2019). Brain tumour segmentation using convolutional neural network with tensor flow. Asian Pacific journal of cancer prevention: APJCP, 20(7), 2095.

[26] Seetha, J., & Raja, S. S. (2018). Brain tumor classification using convolutional neural networks. Biomedical & Pharmacology Journal, 11(3), 1457.

[27] Borole, V. Y., Nimbhore, S. S., & Kawthekar, D. S. S. (2015). Image processing techniques for brain tumor detection: A review. International Journal of Emerging Trends & Technology in Computer Science (IJETTCS), 4(5), 2.

[28] Gooya, A., Pohl, K. M., Bilello, M., Cirillo, L., Biros, G., Melhem, E. R., & Davatzikos, C. (2012). GLISTR: glioma image segmentation and registration. IEEE transactions on medical imaging, 31(10), 1941-1954.

[29] Manikis, G. C., Emmanouilidou, D., Sakkalis, V., Graf, N., & Marias, K. (2011, November). A fully automated image analysis framework for quantitative assessment of temporal tumor changes. In 2011 E-Health and Bioengineering Conference (EHB) (pp. 1-6). IEEE.

[30] Bauer, S., May, C., Dionysiou, D., Stamatakos, G., Buchler, P., & Reyes, M. (2011). Multiscale modeling for image analysis of brain tumor studies. IEEE transactions on biomedical engineering, 59(1), 25-29.

[31] Roy, S., Nag, S., Maitra, I. K., & Bandyopadhyay, S. K. (2013). A review on automated brain tumor detection and segmentation from MRI of brain. arXiv preprint arXiv:1312.6150.

[32] Sindhushree, K. S., Manjula, T. R., & Ramesha, K. (2013). Detection and 3D reconstruction of Brain Tumor from Brain MRI images. International Journal of Engineering Research & Technology (IJERT), 2(8), 528-534.

[33] Krol, A., & Gimi, B. (2017, March). Medical Imaging 2017: Biomedical Applications in Molecular, Structural, and Functional Imaging. In Society of Photo-Optical Instrumentation Engineers (SPIE) Conference Series (Vol. 10137).

[34] Huang, G., Liu, Z., Van Der Maaten, L., & Weinberger, K. Q. (2017). Densely connected convolutional networks. In Proceedings of the IEEE conference on computer vision and pattern recognition (pp. 4700-4708).

[35] He, K., Zhang, X., Ren, S., & Sun, J. (2016). Deep residual learning for image recognition. In Proceedings of the IEEE conference on computer vision and pattern recognition (pp. 770-778).

[36] Alsaif, H., Guesmi, R., Alshammari, B. M., Hamrouni, T., Guesmi, T., Alzamil, A., & Belguesmi, L. (2022). A Novel Data Augmentation-Based Brain Tumor Detection Using Convolutional Neural Network. Applied Sciences, 12(8), 3773.